1990-05

Refractive turbulence profiling using an orbiting lightsource

Krause-Polstorff, J.

Refractive turbulence profiling using an orbiting light source

J. Krause-Polstorff and Donald Walters

The possibility of obtaining vertical profiles of refractive turbulence C_n^2 using an orbiting monochromatic light source is examined. The method employs spatial and temporal filtering of the observed scintillation pattern arising from density fluctuations in the atmosphere to measure C_n^2. The impact of atmospheric motion on the method is discussed along with ways to mitigate its effect. Single and array receiver configurations are examined and the multiple response problem inherent in array configurations is corrected by tuning the individual array elements to the array response. The method is expected to be significantly better than the existing stellar scintillometer method.

I. Introduction

The problem of determining the profile of refractive turbulence has been of considerable interest in determining the performance of ground based optical systems. A double star technique has been discussed by Wang *et al.*[1] and this method has been employed by Roddier[2] to obtain reasonable results for a number of atmospheric layers. A deficiency of this method is the need to have a suitable optical binary source. Ochs *et al.*[3,4] have designed and constructed a refractive scintillometer to determine the vertical profile of the refractive index turbulence from ground based measurements of stellar scintillations. This device has not been free of problems[4–6] and we find that the theoretical derivation for the performance of the 1-D filter on a circular aperture is flawed. The covariance expression with a J_0 Bessel function is incorrect as it assumes a radial spatial variation whereas the spatial variation observed by the filter is 1-D. If one assumes a square as a first approximation to the circular aperture, the J_0 Bessel function is replaced by a cosine function. The circular aperture with a 1-D spatial filter can be consistently handled via an exact expression, however.[7] The main problems of the method are the appreciable overlap of the weighting functions and that the broad peaks of the functions can appreciably degrade the measured vertical profile of C_n^2, the refractive structure constant. A study by Stebbins has examined the problem of layer interdependence in the C_n^2 profiles obtained by the method.[8]

The launch of the relay mirror satellite[9] affords the opportunity of having a moving monochromatic 820-nm laser diode source[10] with a spherically diverging wave function which allows the use of temporal filtering as well as spatial filtering to improve the height resolution of a ground based instrument in determining the refractive index structure parameter as a function of height. We reexamine a method discussed by Clifford and Churnside[11] that used an airplane as a synthetic aperture source. We supplement the original analysis and suggest the possible usefulness of the method when using a satellite source. In particular the problems of multiple height response and crosswind are addressed.

II. Theory

A physically appealing derivation for the log-amplitude fluctuations in the weak refractive turbulence case is due to Lee and Harp[12] and uses the concept of a random phase screen. The log-amplitude fluctuations due to the moving refractive turbulence irregularities in a vertical optical path can be obtained by modeling the refractive field as consisting of a sequence of layers (perpendicular to the direction of propagation). Each layer is made up of 2-D Fourier components $\mathbf{K}$, which are modeled as a phase screen. The light source is in motion parallel to the receiving plane with velocity $\mathbf{v}_s$ at a height h (see Fig. 1). A wave scattered at a height z due to a sinusoidal Fourier component $\mathbf{K}(z)$ reaches the receiving plane as $\mathbf{K}'(z) = \mathbf{K}(z)(1 - z/h)$ which is the geometric projection of $\mathbf{K}$ on the receiving plane. The log-amplitude fluctuation at the receiver due to a single phase screen[11] with a transverse velocity $\mathbf{v}_l$ is:

The authors are with U.S. Naval Postgraduate School, Physics Department, Monterey, California 93943. Sponsored in part by the ASEE/ONT

Received 2 November 1989.

$$d\chi(\rho_1,\rho_2,z,t) = h\,dz\,\sin\left[\frac{K^2 z(h-z)}{2kh}\right](d\nu(\mathbf{K},z)$$
$$\times \exp\{i[\mathbf{K}\cdot\rho_1(1-z/h) + \mathbf{K}\cdot(\rho_2 - \mathbf{v}_s t)z/h + \mathbf{K}\cdot\mathbf{v}_l t]\}$$
$$+ d\nu(-\mathbf{K},z)\exp\{-i[\mathbf{K}\cdot\rho_1(1-z/h)$$
$$+ \mathbf{K}\cdot(\rho_2 - \mathbf{v}_s t)z/h + \mathbf{K}\cdot\mathbf{v}_l t]\}). \quad (1)$$

The point source location is specified by (ρ_2,h) at $t = 0$ and the receiver location by $(\rho_1,0)$ with $d\nu(\pm\mathbf{K},z)$ the Fourier-Stieltjes amplitude of the refractive turbulence with wavenumber $\mathbf{K}$ at height z. The expression obtained above relates the influence of one random phase screen at a layer height z. To obtain the total log-amplitude fluctuation due to the turbulence an integration over all heights and spatial wavenumbers is required.

The receiver on the ground uses a spatial filter (first suggested by Lee[13]) which is sensitive to only a small band around the spatial wavenumber $\mathbf{K}_r \simeq \mathbf{K}(z)(1 - z/h)$ of the filter. The filtered log-amplitude χ_f at the receiver is given by

$$\chi_f(\rho_1\rho_2,t) = \int d^2\rho_1' f_r(\rho_1' - \rho_1)\int_0^h \int d\chi(\rho_1',\rho_2,z), \quad (2)$$

where f_r represents the spatial filter at the receiving aperture. The integrals sum the phase screens of the relevant sinusoidal Fourier components $\mathbf{K}$ in each layer and these are then summed over the propagation path to take into account all atmospheric layers in the path. Integrating $d\chi$ over the filtered aperture f_r is not strictly valid[2] since the intensity not the log-amplitude is aperture averaged. However, in the case of the weak scattering approximation, $dI \simeq 2I_0 d\chi$, where I_0 is the mean intensity so we may proceed by working with the log-amplitude.

The time-lagged covariance of the log-amplitude χ_f is given by

$$C_{\chi_f}(\tau) = \langle[\chi_f(0) - \langle\chi_f(0)\rangle][\chi_f^*(\tau) - \langle\chi_f^*(\tau)\rangle]\rangle, \quad (3)$$

where we have used the idea of a stationary random function to eliminate the explicit t dependence.[14] Inserting Eqs. (1) and (2) into Eq. (3) with $\langle\chi_f\rangle = 0$ for the case of weak refractive turbulence gives

$$C_{\chi_f}(t) = k^2\int d^2\rho_1' f_r(\rho_1' - \rho_1)\int d^2\rho_1'' f_r(\rho_1'' - \rho_1)\int_0^h dz_1\int_0^h dz_2$$
$$\times\iint\langle\{d\nu(\mathbf{K},z_1)\exp(i\zeta_1) + d\nu(-\mathbf{K},z_1)\exp(-i\zeta_1)\}$$
$$\times\{d\nu^*(\mathbf{K}',z_2)\exp(-i\zeta_2) + d\nu^*(-\mathbf{K}',z_2)\exp(i\zeta_2)\}\rangle \quad (4)$$

where

$$\zeta_1 = \mathbf{K}\cdot\rho_1'(1 - z_1/h) + \mathbf{K}\cdot\rho_2$$
$$\zeta_2 = \mathbf{K}'\cdot\rho_1''(1 - z_2/h) + \mathbf{K}'\cdot(\rho_2 - \mathbf{v}_s\tau)z_2/h + \mathbf{K}'\cdot\mathbf{v}_l\tau.$$

For a homogeneous random process[15]

$$\langle d\nu(\mathbf{K},z_1)d\nu^*(\mathbf{K}',z_2)\rangle = \delta(\mathbf{K} - \mathbf{K}')F_n(\mathbf{K},z_1 - z_2)d^2\mathbf{K}d^2\mathbf{K}', \quad (5)$$

where F_n is the 2-D spatial spectral density of the refractive index fluctuations. The Markov approximation can be invoked to further simplify Eq. (4) although it is not strictly valid. The validity of the approximation arises from the fact that the correlation of the refractive index in the z-direction has little effect on the fluctuation characteristics of the wave.[16] The Markov approximation states that

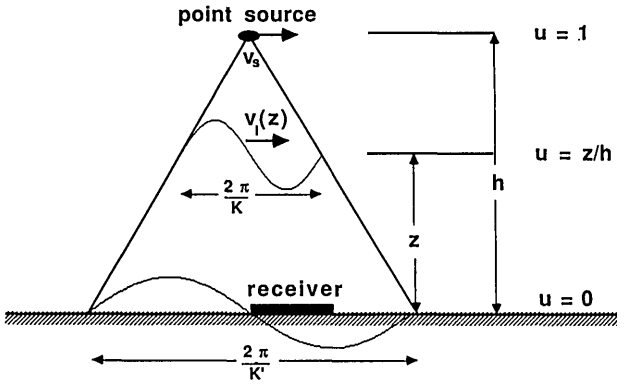

Fig. 1. Moving point source at a height h illuminating a single Fourier component $\mathbf{K}$ of the refractive field at a path position z causes amplitude and phase fluctuations on the ground at $z = 0$. The spatial wavenumber $\mathbf{K}$ is geometrically projected onto the ground so that $\mathbf{K}' = \mathbf{K}(1 - z/h)$. The receiver on the ground uses a spatial filter which is sensitive to only a small band around the spatial wavenumber $\mathbf{K}_r = \mathbf{K}'$.

$$F_n(\mathbf{K},z_1 - z_2) = 2\pi\delta(z_1 - z_2)\Phi_n(\mathbf{K},0), \quad (6)$$

where $\Phi_n(\mathbf{K},0)$ is the 3-D spectral density of the refractive index fluctuations in the plane perpendicular to the propagation. Using Eqs. (5) and (6) in Eq. (4) we obtain

$$C_{\chi_f}(\tau) = 4\pi k^2 h\int_0^1 du\int d^2\mathbf{K}\Phi_n(\mathbf{K},u)\sin^2\left[\frac{K^2 hu(1-u)}{2k}\right]$$
$$\times|F_r[\mathbf{K}(1-u)]|^2\cos[\mathbf{K}\cdot(\mathbf{v}_s\tau u - \mathbf{v}_l\tau)] \quad (7)$$

with $u = z_1/h$ and F_r is the 2-D forward Fourier transform of the spatial filter with positive exponential kernal

$$F_r(\lambda) = \int d^2\rho\exp(i\lambda\cdot\rho)f_r(\rho). \quad (8)$$

The power spectral density $S_{\chi_f}(\omega)$ is the Fourier transform of the correlation function

$$S_{\chi_f}(\omega) = \frac{1}{2\pi}\int_{-\infty}^{\infty} d\tau\exp(-i\omega\tau)C_{\chi_f}(\tau), \quad (9)$$

and this gives as the power spectral density of the log-amplitude fluctuations:

$$S_{\chi_f}(\omega) = 2\pi k^2 h\int_0^1 du\int d^2\mathbf{K}\sin^2\left[\frac{K^2 hu(1-u)}{2k}\right]\Phi_n(\mathbf{K},u)$$
$$\times|F_r[\mathbf{K}(1-u)]|^2\{\delta[\omega + \mathbf{K}\cdot(\mathbf{v}_s u - \mathbf{v}_l)]$$
$$+ \delta[\omega - \mathbf{K}\cdot(\mathbf{v}_s u - \mathbf{v}_l)]\}. \quad (10)$$

Before examining realistic spatial filter configurations it is instructive to look at the effect of a perfect spatial filter sensitive to only one spatial wavenumber $\mathbf{K}$ in the x-direction and uniform response in the y-direction,

$$|F_H|^2 \propto \tfrac{1}{2}\delta[K_y(1-u)]\{\delta[K_x(1-u)-K_r]+\delta[K_x(1-u)+K_r]\}, \tag{11}$$

where the x and y subscripts refer to the respective components of the spatial wavenumbers. Integration over K_y leaves us with

$$\begin{aligned} S_{\chi_f}(\omega) \propto \pi k^2 h \int_0^1 \frac{du}{(1-u)} \int_{-\infty}^{\infty} dK_x \Phi_n(K_x,u) \sin^2\left[\frac{K_x^2 hu(1-u)}{2k}\right] \\ \times \{\delta[K_x(1-u)-K_r]+\delta[K_x(1-u)+K_r]\} \\ \times \{\delta[\omega+K_x(v_{sx}u-v_{lx})]+\delta[\omega-K_x(v_{sx}u-v_{lx})] \end{aligned} \tag{12}$$

noting that only the x-components of $\mathbf{v}_s$ (source velocity) and $\mathbf{v}_l$ (layer velocity) survive the integration to contribute to the power density spectrum. Multiplication of the delta functions yields four terms which combine into two terms because of the symmetry of the integral under the transformation $K_x \rightarrow -K_x$ to yield

$$\begin{aligned} S_{\chi_f}(\omega) = 2\pi k^2 h \int_0^1 \frac{du}{1-u} \int_0^{\infty} dK_x \Phi_n(K_x,u) \sin^2\left[\frac{K_x^2 hu(1-u)}{2k}\right] \\ \times \left\{\frac{1}{|\omega+K_r v_{sx}|}\delta\left[K_x-\left(\frac{\omega+K_r v_{sx}}{v_{sx}-v_{lx}}\right)\right]\delta\left[u-\left(\frac{\omega+K_r v_{lx}}{\omega+K_r v_{sx}}\right)\right]\right. \\ \left. + \frac{1}{|\omega-K_r v_{sx}|}\delta\left[K_x+\left(\frac{\omega-K_r v_{sx}}{v_{sx}-v_{lx}}\right)\right]\delta\left[u-\left(\frac{\omega-K_r v_{lx}}{\omega-K_r v_{sx}}\right)\right]\right\}, \end{aligned} \tag{13}$$

where the second term in the sum contributes only if $v_{sx} > v_{lx} > \omega/K_r$. Note that we assume $v_{sx} > v_{lx}$ and have taken $v_l \approx$ constant whereas in reality the layer velocity is a function of u. Evaluating the integral in Eq. (13) assuming $\omega > K_r v_{lx}$ (ie., the second term does not contribute) we find that

$$S_{\chi_f} \propto \frac{4\pi k^2 h}{K_r(v_s-v_l)} \Phi(K_0,u_0) \sin^2\left[\frac{K_r h(\omega+K_r v_l)}{2k(v_s-v_l)}\right], \tag{14}$$

with

$$K_0 = \frac{\omega+K_r v_s}{v_s-v_l},$$

and the probed height

$$u_0 = \frac{\omega+K_r v_l}{\omega+K_r v_s},$$

with v_s and v_l the x-components of the source and layer velocities. The quantity K_0 is the magnitude of the wavenumber at the probed height u_0 so that $K_r = K_0(1-u_0)$. Note the dependence of u_0 on the layer velocity. The layer velocity can be neglected if $v_s \gg v_l$ and $\omega/K_r v_l \gg 1$.

In the remainder of this paper we use the Kolmogorov spectrum for turbulence:

$$\Phi_n(K_x,K_y,u) = 0.033 C_n^2(u)(K_x^2+K_y^2)^{-11/6}. \tag{15}$$

III. Array Receiver

Clifford and Churnside[11] have considered two practical implementations for a receiving system. The first we shall consider is an array of receivers (telescopes). Taking the array to be a zero-sum receiver we have an array of N (even) circular apertures spaced a distance d apart. The filter function is given by the convolution of the circular aperture with a sum of delta functions located at the receiver locations (array theorem).[15] The transform of the filter function is easily determined via the convolution theorem and is merely the product of the individual transforms. We obtain for the filter function transform squared

$$|F_H|^2 = \left|\frac{2J_1[r(1-u)\sqrt{K_x^2+K_y^2}]}{Nr(1-u)\sqrt{K_x^2+K_y^2}} \frac{\sin[N/2\,K_x(1-u)d]}{\cos[K_x/2(1-u)d]}\right|^2, \tag{16}$$

where r is the radius of the individual apertures. If the array is oriented along the velocity component of the source $\mathbf{v}_s$ ($=v_{sx}$) and we neglect the layer velocities, $|F_H|^2$ is given by

$$|F_H|^2 = \left|\frac{2J[r(1-u)\sqrt{(\omega/v_s u)^2+K_y^2}]}{r(1-u)\sqrt{(\omega/v_s u)^2+K_y^2}} \frac{\sin[N\omega d(1-u)/2v_s u]}{\cos[\omega d(1-u)/2v_s u]N}\right|^2, \tag{17}$$

where the second factor (which we shall call B) represents the transform of the array of delta functions and can be rewritten more informatively as

$$B = \frac{\sin\left[\frac{N\pi}{2}\left(\frac{u_0}{1-u_0}\right)\left(\frac{1-u}{u}\right)\right]}{\cos\left[\frac{\pi}{2}\left(\frac{u_0}{1-u_0}\right)\left(\frac{1-u}{u}\right)\right]} \tag{18}$$

with the normalized probed path position given by

$$u_0 = \frac{\omega d}{\omega d + \pi v_s}. \tag{19}$$

Note that the N in the denominator of Eq. (17) [compare Clifford and Churnside Eq. (45)] is necessary for proper normalization of the spectral density of the log-amplitude fluctuations. The factor $|B|$ approaches N as $u \rightarrow u_0$ but $|B|$ goes to N for:

$$u_n \rightarrow \frac{u_0}{2n(1-u_0)+1}, \qquad n = 0,1,2,\ldots \tag{20}$$

This means there are peaks at heights $<u_0$ modulated by the single aperture function (i.e., see Figs. 2–5).

In the figures we plot the normalized weighting function $W(u)/W(u_0)$ where:

$$\begin{aligned} W(u) = \int dK_y |F_H|^2 \sin^2\left[\frac{[(\omega/v_s u)^2+K_y^2]hu(1-u)}{2k}\right] \\ \times \frac{\Phi_n(\omega/v_s u, K_y, u)}{u}. \end{aligned} \tag{21}$$

For the purposes of illustration we shall look at an example used by Clifford and Churnside[11] with $u_0 = \frac{1}{2}$, $r = 0.05$ m, $d = 1$ m, and $\omega = 100\pi$. The source is at a height of 1 km and moving with a velocity of 100 m/s in level flight. In Fig. 2 the peak for $n = 1$ has a height 70% of that of the main peak ($n = 0$) which makes the configuration unreliable to use for sensing C_n^2 near midpath and unusable for positions near the source as shown in Fig. 3 for $u_0 = \frac{7}{8}$, $d = 7$ m, and $\omega = 100\pi$. This

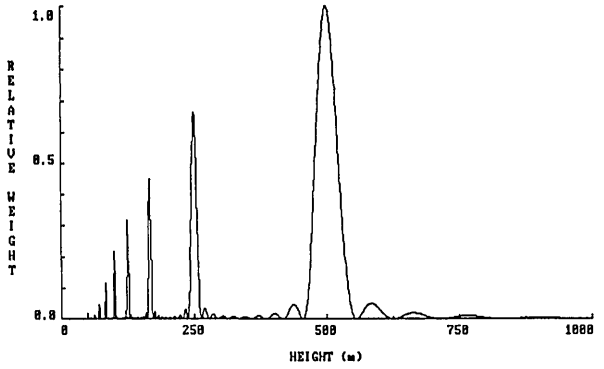

Fig. 2. Weighting function for a point source moving parallel to ten element array receiver with $v_s = 100$ m/s, $h = 1000$ m, $\omega = 100\pi$, $d = 1$ m, $r = 0.05$ m, and $u_0 = 1/2$. Note the peaks of the weighting function at heights less than midpath.

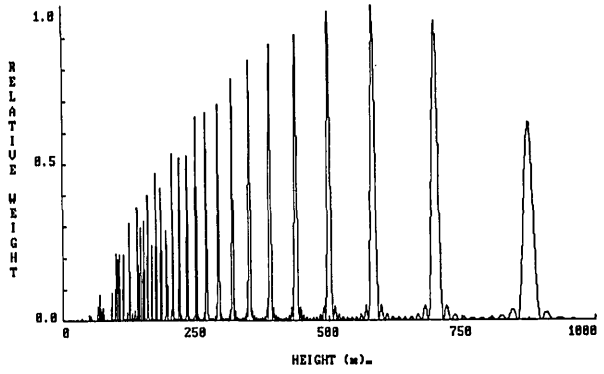

Fig. 3. Weighting function with configuration as in Fig. 2 except $d = 7$ m and $u_0 = 7/8$. Normalization is to u_3 peak. The problem of multiple peaks is very evident.

problem can be avoided if the single aperture and temporal filter are tuned to suppress the extra peaks. We note the improvement in Fig. 4 where $u_0 = 7/8$, but $d = 0.1$ m, and $\omega = 7000\pi$. We choose this example merely for purposes of illustration. The single aperture is made to probe the same height as the entire array and the peaks to the left of the height of interest are effectively eliminated. Figure 5 shows the weighting function for the tuned single aperture relevant to Fig. 4. Next we examine the effect of a layer velocity $\mathbf{v}_l$ along the x-axis on the weighting function. For a value of $u_0 = 1/2$ with a layer velocity of 20 m/s parallel to the x-component of the source velocity the pattern of Fig. 2 is shifted $0.2u_0$ to the right as shown in Fig. 6. The magnitude of the weighting function is also affected. A component of layer velocity along the array introduces an uncertainty into the weighting and the height which is being probed from the ground because $\mathbf{v}_l$ is in general not known. The resonances are shifted to the right (if the wind were antiparallel the shift would be to the left) in the figures to a new value u_{ns}:

$$u_{ns} = u_n + (1 - u_n)v_{lx}/v_s. \tag{22}$$

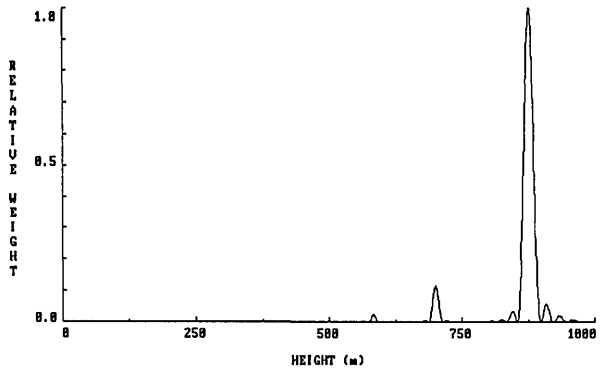

Fig. 4. Weighting function with configuration as in Fig. 3 but $d = 0.1$ m and $\omega = 7000\pi$, so that again $u_0 = 7/8$. The multiple peaks are effectively eliminated due to the tuning of the single aperture to the same height as the array.

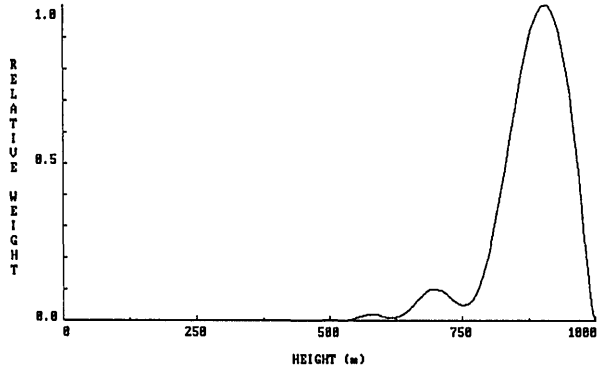

Fig. 5. Weighting function for single aperture = 0.05 m tuned to $u_0 = 7/8$. This function forms the envelope for the weighting function in Fig. 4.

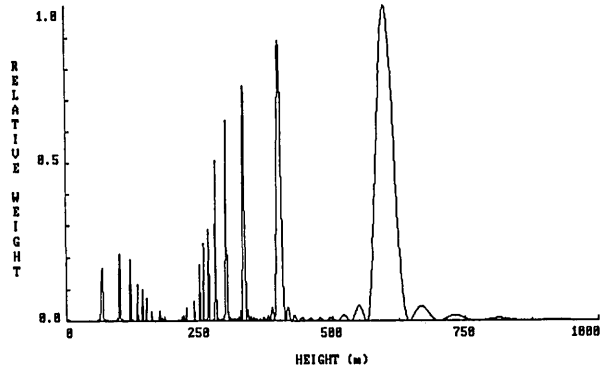

Fig. 6. Weighting function as in Fig. 2 but with a uniform wind velocity $\mathbf{v}_l = 20$ m/s along the receiver array parallel to point source velocity $\mathbf{v}_s = 100$ m/s. Note that the peak of the weighting function is moved ~100 m above midpath and that there is essentially no response at $u_0 = 1/2$.

As one would expect from geometric considerations the layer velocity has the least effect for those layers closest to the transmitter. The effect of the wind component perpendicular to the array for $u_0 = 1/2$ and $v_{ly} = 20$ m/s (other values as in Fig. 2) can be seen in

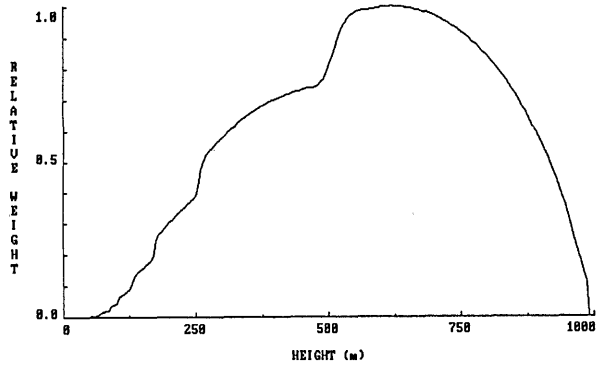

Fig. 7. Disruption of weighting function with configuration as in Fig. 2 by a 20-m/s wind perpendicular to point source velocity. The weighting function resembles that of a single aperture.

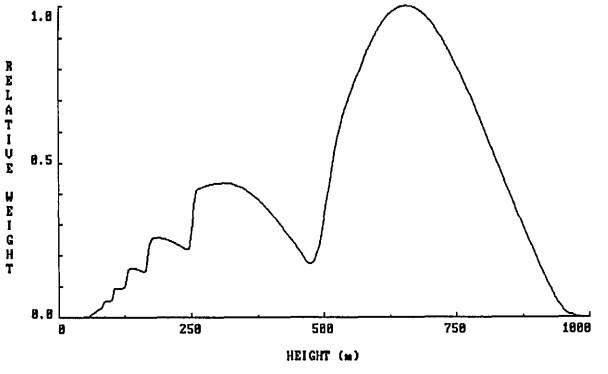

Fig. 8. Same as Fig. 7 but with only a 5-m/s crosswind. It is apparent that even a slight crosswind can seriously degrade the weighting function of the configuration.

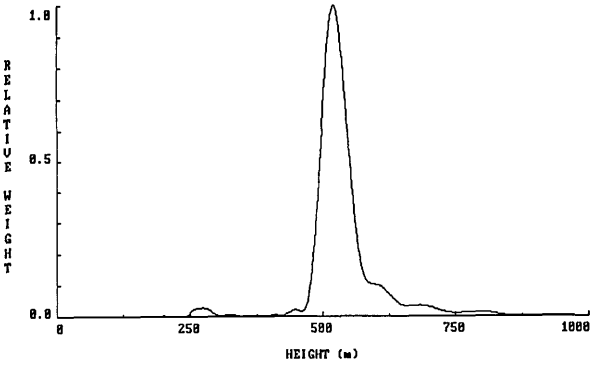

Fig. 9. Weighting function for $u_0 = \frac{1}{2}$ with a ten element array of elliptical apertures having a major axis = 0.15 m and a minor axis = 0.05 m. d = 0.1 m, and $\omega = 1000\pi$. The crosswind is 20 m/s. The elliptical receiver elements stabilize the weighting function against crosswind.

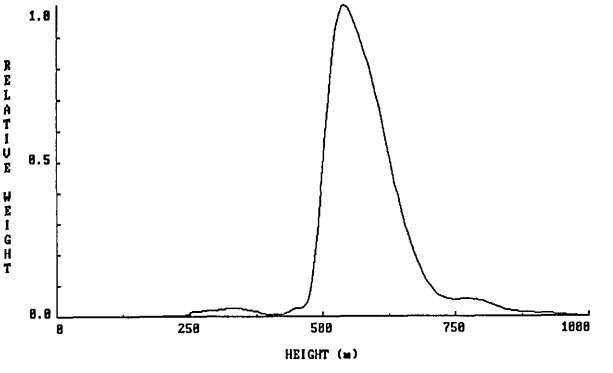

Fig. 10. Same as in Fig. 9 but with the elliptical apertures replaced by circular ones. Although the weighting function is broader the dense packing used to suppress the multiple peaks also serves to stabilize the weighting function against crosswinds. Here v_s = 20 m/s.

Fig. 7 where the weighting function has been totally disrupted. The crosswind introduces a K_y dependence into K_x. The weighting function is now similar to that of a single circular aperture. Even a moderate crosswind of 5 m/s produces an appreciable degradation of the weighting function (see Fig. 8). The crosswind sensitivity of the array can be reduced if the individual aperture extent in the y-direction is larger than the spacing d of the apertures in the array. Fig. 9 illustrates the effect of a 20-m/s crosswind (y-direction) on the (n =)10 elliptical apertures with a 0.3-m extent in the y-direction and a spacing between apertures of d = 0.1 m. Individual aperture width is also 0.1 m but $\omega = 1000\pi$. This dense pack configuration has the single apertures tuned to suppress the peaks $<u_0$ and also aids in reducing sensitivity to crosswind because the spacing d between elements of the linear array is reduced to a minimum. The tuning is not quite exact for circular or elliptical apertures in the dense pack configuration because of the circular geometry involved. It is exact however if one takes rectangular apertures as is clear by looking at the relevant analytic expression. Figure 10 is the same configuration as in Fig. 9 except that the apertures are circular with a diameter of 0.1 m. The broad character of the weighting function in Fig. 10 shows it is limited not by the number of elements in the array but by the contribution of K_y component in the integration which leads to a superposition of shifted peaks (smearing of the resonance peak). The effective long wavelength of the array in the y-direction for the elliptical aperture gives an approximate delta function response in K_y (i.e., response only to smallest K_y values). The example for perfect filters in the beginning of the paper implies infinite extent in the x and y-directions and therefore masks the problem caused by winds in the y-direction for real spatial filters. The filter frequency ω can be reduced by enlarging the aperture and therefore increasing the array spacing but this comes at the cost of decreasing the strength of the fluctuations (the aperture averaging effect).

So far we have examined the usefulness of probing the atmosphere at or above midpath with a multiaperture array system and synthetic aperture source. In the event that the synthetic aperture source is an orbiting satellite we shall be interested not in probing at

midpath but at significantly lower portions of the optical path. The satellite is assumed to be in a circular orbit at a height of 500 km. Hence, the interesting values of u_0 are very small. The spatial resolution of the weighting function for the multiple aperture system at a height u_0 is found by an expansion of the trigonometric function arguments about u_0 giving

$$|F[\mathbf{K}(1-u)]|^2 = \left| \sum_{n=-\infty}^{n=\infty} 2\,\mathrm{sinc}\left[\frac{(2n+1)\pi}{2}\right] \exp[i(2n+1)K_r\Delta] \times J_{1c}\left[r\sqrt{\left\{\frac{\pi}{d}\left(\left(\frac{u_0}{1-u_0}\right)\left(\frac{1-u}{u}\right) \mp (2n+1)\right)\right\}^2 + K_y^2(1-u)^2}\right]\right|^2 . \quad (28)$$

$$B = \frac{\sin^2\left[\frac{N\pi(u-u_0)}{2u_0(1-u_0)}\right]}{\sin^2\left[\frac{\pi(u-u_0)}{2u_0(1-u_0)}\right]} . \quad (23)$$

The spatial resolution of the resonance is

$$\sigma_u = \frac{2u_0(1-u_0)}{N} . \quad (24)$$

At low altitudes (small u_0) for a ten element zero sum receiver the spatial resolution is $\sim 1/5$ of the layer height. The spatial resolution for the peaks to the left of the main resonance (for small u_0) is approximately

$$\sigma_{u_n} \approx \frac{2u_0}{N(2n+1)} , \quad (25)$$

which indicates they can detract from the performance of the method. Another way to reduce the effect of multiple peaks is to choose different aperture sizes to probe different heights. In this way the response of the aperture function to different heights modulates the response of the filter (e.g., a small aperture suppresses lower heights less than a large aperture for a given filter frequency).

IV. Single Receiver

The second receiver configuration is a single round aperture receiver subdivided into stripes which are alternately reflecting and transmitting leading to a zero-sum receiver. We chose to work with the exact filter function and its transform as given by Churnside *et al.*[7]

$$|F[\mathbf{K}(1-u)]|^2 = \left| \sum_{n=-\infty}^{n=\infty} 2\,\mathrm{sinc}\left[\frac{(2n+1)\pi}{2}\right] \exp[i(2n+1)K_r\Delta] \times J_{1c}(r\sqrt{K_x(1-u) - (2n+1)K_r)^2 + K_y^2(1-u)^2})\right|^2 , \quad (26)$$

where $J_{1c}(x) = J_1(x)/x$, r is the aperture radius and K_r is the filter frequency π/d (d = stripe width). The Δ represents a phase shift of the filter pattern (stripes) The + sign applies for negative values of n. The from a centered transmitting (or reflecting stripe). In this case the probed path position u_0 is

$$u_n = \frac{\omega d}{\omega d + (2n+1)\pi v_s} , \quad (27)$$

for $n = 0$. This is a slightly different formulation of Eq. (19) to include the other probed heights as well. We can rewrite the filter function in terms of u_0 to give

spatial resolution afforded by this filter function is approximately:

$$\sigma_u \approx \frac{3.8317 d u_0(1-u_0)}{\pi r} , \quad (29)$$

where the numerical constant comes from the first zero of the J_1 Bessel function.

V. Implementation

In Fig. 11 we show the weighting function for the spatially filtered single aperture receiver probing at $u_0 = 1/2$ with the moving source having a velocity of 100 m/s at a height of 1 km. Here the aperture radius $r = 0.2$ m, the stripe width $d = 0.1$ m, and the frequency $\omega = 1000\pi$. In the event of an orbiting light source at ~500-km altitude the filtered single aperture is most appropriate for probing atmospheric layers up to ~4 km in height. A major advantage of the single aperture receiver is its inherent insensitivity to crosswinds. For heights appreciably greater than this value the aperture must be larger than the 0.2-m radius telescopes commonly available. Figs. 12–16 show various weighting functions obtained for heights from 1–5.2 km. Figure 16 shows the weighting function for 5.2 km which is quite broad and suggests that an array receiver would give substantially better height resolution here. More spatial cycles across a larger aperture would improve the height resolution as well (r/d for single aperture $\simeq N$ for array). If multiple peaks are a problem with the single aperture receiver, (see Fig. 11) a variation of the weighting function approach of Ochs *et al.*[1] could be employed to reduce their impact. The major unwanted contribution to the weighting function comes from the first peak to the left of the u_0 peak which can be eliminated by subtracting the output of a complementary receiver with stripe width

$$d_n = \frac{\pi u_0 v_s}{(2n+1)\omega(1-u_0)} , \quad (30)$$

where $n = 1$.

For the single aperture receiver operating at $\omega = 800\pi$ the power spectral density at 1 km is:

$$S_{x_f} = 5.9 \times 10^7 [\mathrm{m}^{2/3}\mathrm{s}] C_n^2 \quad (31)$$

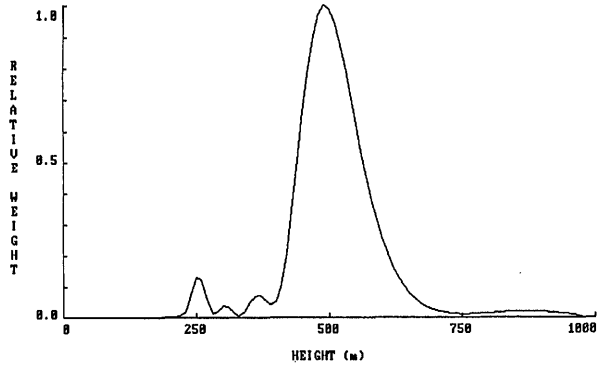

Fig. 11. Weighting function for a single spatially filtered receiver with $r = 0.2$ m, $\omega = 1000\pi$, and $K_r = 2\pi/0.2$ m. The probed height is 500 m or $u_0 = \frac{1}{2}$. The source is at 1 km moving with a velocity of 100 m/s.

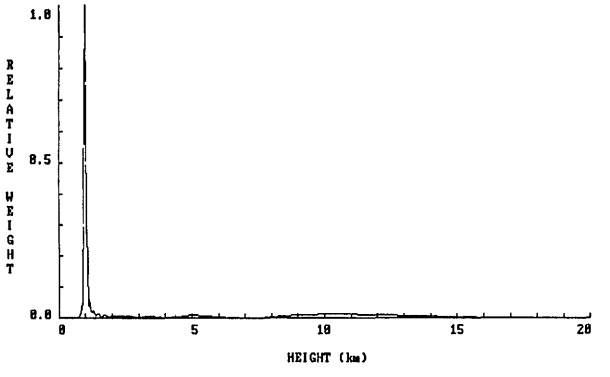

Fig. 12. Weighting function for single receiver with $r = 0.2$ m, $\omega = 800\pi$, and $K_r = 2\pi/0.0375$ m. The source is taken to be an orbiting satellite at 500 km height. Here $u_0 = 0.002$.

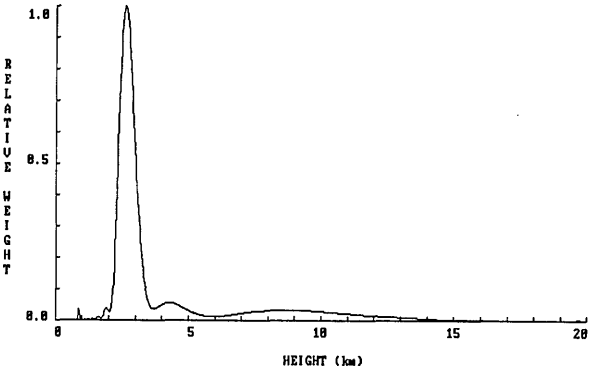

Fig. 13. Weighting function for configuration as in Fig. 12 but $K_r = 2\pi/0.1$ m. The probed height is $u_0 = 0.0054$.

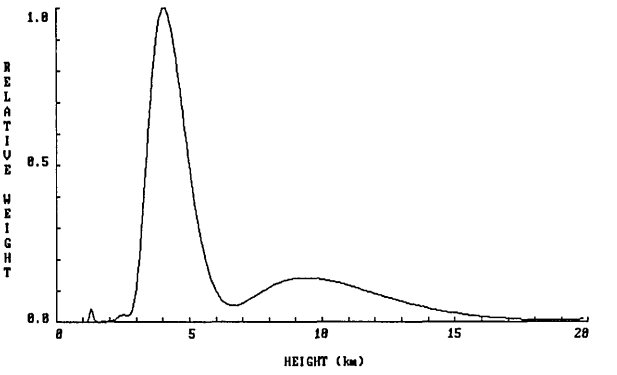

Fig. 14. Weighting function for configuration as in Fig. 12 but $K_r = 2\pi/0.15$ m. The probed height is 4050 m. Note the hump to the right of the main weighting function.

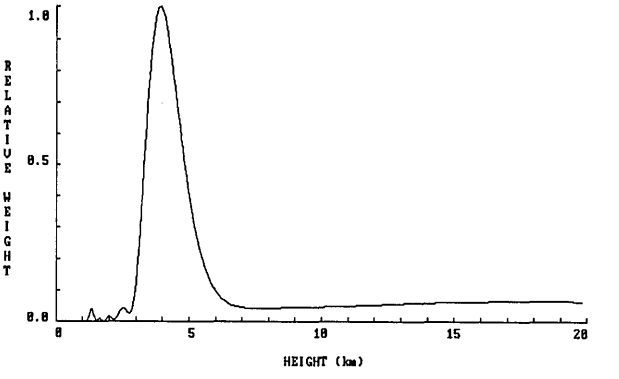

Fig. 15. Identical setup as in Fig. 14 except that the spatial filter is phase shifted $\pi/2$ relative to the aperture (see text). Note the absence of the hump relative to the previous Fig. 14.

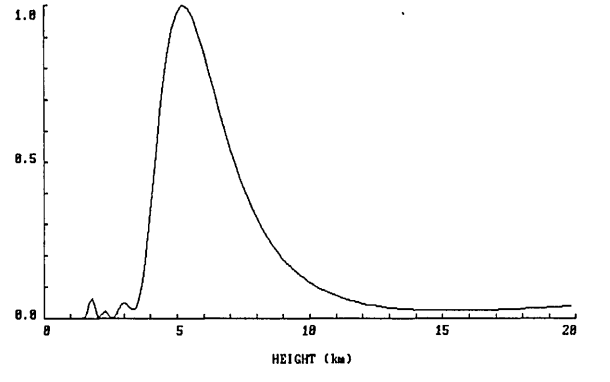

Fig. 16. Weighting function for single spatially filtered receiver with $r = 0.2$ m, $\omega = 800\pi$, $K_r = 2\pi/0.2$ m, and $u_0 = 0.0104$. Note the broad character of the weighting function as the aperture can accommodate only one wavelength. Compare with Figs. 17–19.

and at 5.2 km:

$$S_{\chi_\ell} = 1.2 \times 10^{10}[\mathrm{m}^{2/3}\mathrm{s}]C_n^2 \tag{32}$$

where we have approximated the weighting function by an equivalent triangle. In Figs. 14 and 15 the weighting function is probing a height of 4 km. In Fig. 14 the filter is centered in the aperture and we have a hump to the right of the peak. In Fig. 15 the spatial filter is shifted $\pi/2$ relative to the aperture and the hump has been smoothed out. This illustrates the effect of the phase factor Δ in Eq. (28). A phase shift can be employed in some cases to obtain a weighting

function with a more Gaussian appearance.

An important consideration in the single aperture case is the question of sufficient light striking each stripe. For the worst case example (Fig. 12) we find, assuming a magnitude zero source (10^{-8} W/m^2 flux) that the smallest stripe (assuming a 10% counting efficiency and sampling frequncy of 800 Hz) sees in excess of 100,000 photons during each sampling period. This should be sufficient to suppress shot noise but probably requires some finesse to implement.

To determine the refractive structure constant at heights $\geq$4 km we turn our attention back to the array receiver. Taking the apertures to be 0.05 m in radius and the array to consist of twenty apertures spaced 0.1 m apart we show the weighting functions for heights $\approx$ 3.9 km, 8 km, and 15.2 km in Figs. 17–19 along with the appropriate sampling frequencies. The photon counts can be readily increased by choosing a larger aperture size and adjusting the temporal filter frequency accordingly. To control the crosswind effect these apertures should actually have an elliptical shape with the major axis extending perpendicular to the source direction of motion. A rectangular aperture might also be implementable. At 3.9 km the power spectral density is given by:

$$S_{\chi_f} = 1.1 \times 10^9 [\mathrm{m}^{2/3}\mathrm{s}] C_n^2 \tag{33}$$

with $\omega = 600\pi$. At 15.2 km:

$$S_{\chi_f} = 1.2 \times 10^{10} [\mathrm{m}^{2/3}\mathrm{s}] C_n^2 \tag{34}$$

with $\omega = 2400\pi$. Direct integration of the weighting functions and the Hufnagel C_n^2 profile show good agreement with the triangle estimates in Eqs. (33) and (34).

For implementation one could sample at twice the highest filter frequency and monitor the power spectrum of the fluctuations at the filter frequencies in parallel, thereby simultaneously obtaining data on the refractive structure constant in different layers.

VI. Conclusions

The existence of an orbiting light source should provide a means of measuring the vertical profile of the refractive structure constant to a greater accuracy than is presently possible with the single source stellar scintillometers and would not suffer from the source problems associated with the binary star technique. The method is sensitive to the wind velocity of the various layers probed. In the aperture array configuration there is a degrading by broadening of the weighting function by crosswinds that can be substantially reduced by going to elliptical or rectangular apertures. The array configuration also suffers from response at subharmonics (lower heights than the target height) which can be suppressed by having both the array and individual array aperture sensitive to the same height. Both the single aperture and multiple aperture receivers are sensitive to winds moving parallel to K_r which serve to shift the weighting function to lower or higher altitudes thereby introducing uncertainty into the height profile. Information on wind speed and direction at various heights can be used to compensate for this in the calculated weighting function. Caution must be exercised at the layer being probed so that the projected source velocity is not nearly equal to the wind velocity along the spatial filter (so that K_x is not greater than the upper cutoff of the Kolmogorov spectrum). We find that the single aper-

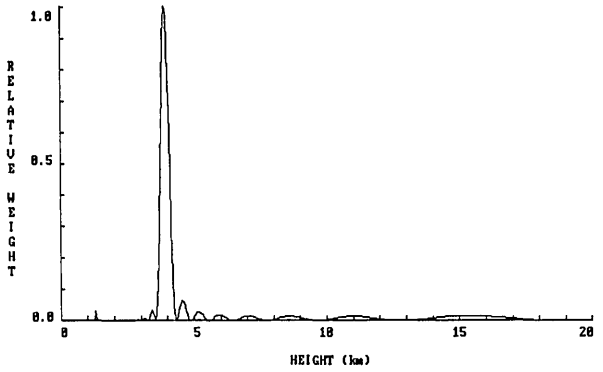

Fig. 17. Array receiver weighting function for satellite source at 500-km height consisting of twenty elements with $r = 0.05$, $d = 0.1$, and $\omega = 600\pi$. The probed height is 3900 m.

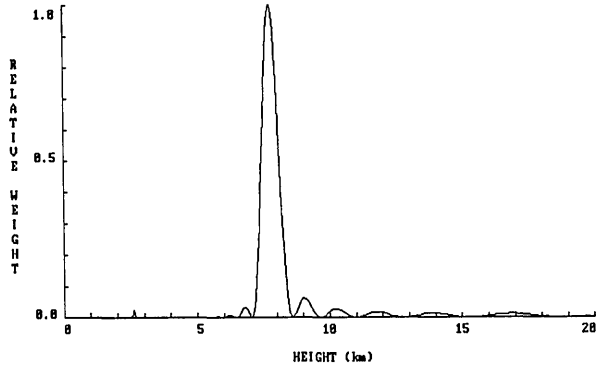

Fig. 18. Configuration as in Fig. 17 but with $\omega = 1200\pi$ and a probed height of 7750 m. Note there is no overlap with weighting function of Fig. 17.

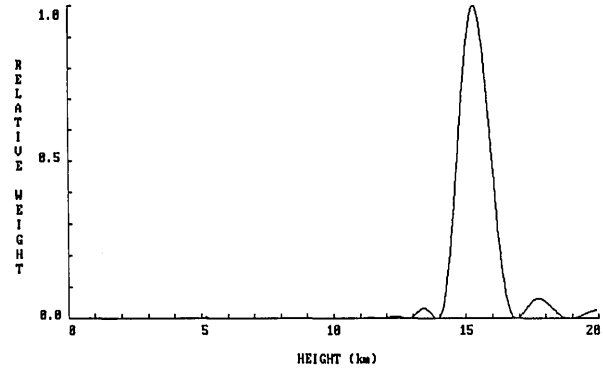

Fig. 19. Configuration as in Fig. 17 but with $\omega = 2400\pi$ and a probed height of 15300 m.

ture system is appropriate for altitudes ≤4 km. At heights >4 km it is advantageous to use the array method as the height resolution of the spatially filtered single aperture system for higher altitudes is poor. The resolution is limited because the practical limit on the single aperture size restricts the number of spatial cycles across the aperture. The layer interdependence problem in this method is expected to be sharply reduced from the existing stellar scintillometer method as the weighting functions are much sharper in the present method.

References

1. T. I. Wang, S. F. Clifford, and G. R. Ochs, "Wind and Refractive-Turbulence Sensing Using Crossed Laser Beams," Appl. Opt. **13,** 2602–2608 (1974).
2. A. Rocca, A. Roddier, and J. Vernin, "Detection of Atmospheric Turbulent Layers by Spatiotemporal and Spatioangular Correlation Measurements of Stellar-Light Scintillation," J. Opt. Soc. Am. **64,** 1000–1004 (1974).
3. G. R. Ochs, T. I. Wang, R. S. Lawrence, and S. F. Clifford, "Refractive-Turbulence Profiles Measured by One-Dimensional Spatial Filtering of Scintillations," Appl. Opt. **15,** 2504–2510 (1976).
4. G. R. Ochs, R. S. Lawrence, and T. I. Wang, "Stellar Scintillation Measurement of the Vertical Profile of Refractive-Index Turbulence in the Atmosphere," in Proc. Soc. Photo-Opt. Instrum. Eng. **75,** (1976).
5. N. Chonacky and R. W. Deuel, "Atmospheric Optical Turbulence Profiling by Stellar Scintillometers: an Instrument Evaluation Experiment," Appl. Opt. **27,** 2214–2221 (1988).
6. G. C. Loos and C. B. Hogge, "Turbulence of the Upper Atmosphere and Isoplanatism," Appl. Opt. **18,** 2654–2661 (1979).
7. J. H. Churnside, R. J. Lataitis, and R. S. Lawrence, "Localized Measurements of Refractive Turbulence Using Spatial Filtering of Scintillations," Appl. Opt. **27,** 2199–2213 (1988).
8. D. Stebbins, "Analysis of Inter-Layer Independence of Stellar Scintillometer Profiles of C_n^2," RADC Technical Report RADC-TR 87-156 (Rome Air Development Center, Griffiss AFB, NY, 1987).
9. P. A. Gilmartin, "SDI Experiments Set For Launch in January," Aviat. Week Space Technol. **131** (No. 11), 35 (1989).
10. Private Communication, Ball Engineering.
11. S. F. Clifford and J. H. Churnside, "Refractive Turbulence Profiling Using Synthetic Aperture Spatial Filtering of Scintillation," Appl. Opt. **26,** 1295–1303 (1987).
12. R. W. Lee and J. C. Harp, "Weak Scattering in Random Media, with Applications to Remote Probing," Proc. IEEE **57,** 375–406 (1969).
13. R. W. Lee, "Remote Probing Using Spatially Filtered Apertures," J. Opt. Soc. Am. **64,** 1295–1303 (1974).
14. A. Papoulis, *Systems and Transforms with Applications to Optics* (McGraw-Hill, New York, 1968).
15. V. I. Tatarskii, *Wave Propagation in a Turbulent Medium* (McGraw-Hill, New York, 1961).
16. A. Ishimaru, *Wave Propagation and Scattering in Random Media* (Academic Press, New York, 1978).